APL Materials

RESEARCH ARTICLE | JUNE 01 2023

Anticorrelated photoluminescence and free charge generation proves field-assisted exciton dissociation in low-offset PM6:Y5 organic solar cells

Special Collection: Advances in Organic Solar Cells

Manasi Pranav ; Thomas Hultzsch; Artem Musiienko ; Bowen Sun ; Atul Shukla ; Frank Jaiser ; Safa Shoaee ; Dieter Neher

APL Mater. 11, 061111 (2023)
https://doi.org/10.1063/5.0151580

Anticorrelated photoluminescence and free charge generation proves field-assisted exciton dissociation in low-offset PM6:Y5 organic solar cells

Cite as: APL Mater. 11, 061111 (2023); doi: 10.1063/5.0151580
Submitted: 23 March 2023 • Accepted: 10 May 2023 •
Published Online: 1 June 2023

Manasi Pranav,[1,2] Thomas Hultzsch,[1] Artem Musiienko,[3] Bowen Sun,[2] Atul Shukla,[1] Frank Jaiser,[1] Safa Shoaee,[2] and Dieter Neher[1,a)]

AFFILIATIONS

[1] Soft Matter Physics and Optoelectronics, Institute of Physics and Astronomy, University of Potsdam, 14476 Potsdam-Golm, Germany
[2] Optoelectronics of Disordered Semiconductors, Institute of Physics and Astronomy, University of Potsdam, 14476 Potsdam-Golm, Germany
[3] Helmholtz-Zentrum Berlin für Materialien und Energie, 12489 Berlin, Germany

Note: This paper is part of the Special Topic on Advances in Organic Solar Cells.
[a)] **Author to whom correspondence should be addressed:** neher@uni-potsdam.de

ABSTRACT

Understanding the origin of inefficient photocurrent generation in organic solar cells with low energy offset remains key to realizing high-performance donor-acceptor systems. Here, we probe the origin of field-dependent free-charge generation and photoluminescence in non-fullereneacceptor (NFA)-based organic solar cells using the polymer PM6 and the NFA Y5—a non-halogenated sibling to Y6, with a smaller energetic offset to PM6. By performing time-delayed collection field (TDCF) measurements on a variety of samples with different electron transport layers and active layer thickness, we show that the fill factor and photocurrent are limited by field-dependent free charge generation in the bulk of the blend. We also introduce a new method of TDCF called m-TDCF to prove the absence of artifacts from non-geminate recombination of photogenerated and dark charge carriers near the electrodes. We then correlate free charge generation with steady-state photoluminescence intensity and find perfect anticorrelation between these two properties. Through this, we conclude that photocurrent generation in this low-offset system is entirely controlled by the field-dependent dissociation of local excitons into charge-transfer states.

I. INTRODUCTION

Free charge generation in organic photovoltaic cells (OPV) critically relies on photoinduced charge transfer between an electron donor (D) and an electron acceptor (A). This is because the binding energy of excitons in organic semiconductors is much larger than thermal energy at room temperature. To reduce energy losses on charge transfer (CT), a small energy offset of the frontier orbitals is desired. For electron (hole) transfer, this pertains to a low offset between the lowest unoccupied molecular orbitals (LUMO) [highest occupied molecular orbitals (HOMO)]. However, if the energy offset is too small, exciton dissociation at the DA heterojunction becomes inefficient. Numerous studies have shown that an offset range of 0.1–0.5 eV is critical to achieve efficient photon-to-free charge conversion. Inefficient exciton dissociation for low-offset systems has been proven by a relatively lower photovoltaic external quantum efficiency (EQE_{PV}), inefficient fluorescence quenching, and reduced free charge generation rates in transient absorption studies.[1–6]

More recently, several papers provided evidence for electric-field-assisted exciton dissociation in low-offset systems.[7–9] For example, Weu *et al.* studied the blend of the donor polymer PffBT4T-2OD with the fullerene-based acceptor $PC_{71}BM$.[8]

Compared with the neat blend films, complete devices exhibited lower steady-state photoluminescence (ssPL) intensity, a faster signal decay in transient photoluminescence (TrPL) measurements, as well as more efficient charge generation in transient absorption (TAS). It was concluded that the presence of a built-in electric field in the device assists dissociation of excitons, which would otherwise decay radiatively. Interestingly, these devices exhibited a high fill factor (FF) of 71.4% despite an active layer thickness of 300 nm. With such a high value of the FF, the photogenerated current saturated within 0.3 V below the open circuit voltage. In other words, a low electric field of $\sim 10^6$ V m^{-1} was sufficient to split almost all excitons. This implies a very small exciton binding energy in this system. Note not only that the use of a different substrate in the full device (ITO) vs the neat film (glass) might affect the blend morphology but also that dark charge carriers injected by the electrodes may have an additional effect on the excitation dynamics in the device. Liu *et al.* studied blends of the donor polymer PTQ10 with two non-fullerene acceptors, ZITI-C or ZITI-N.[7] These combinations were chosen because of their different HOMO-HOMO offsets (50 meV for PTQ10:ZITI-C compared with −70 meV for PTQ10:ZITI-N), the latter of which exhibited a slower hole transfer and a strong bias-dependence of EQE_{PV}. These observations were assigned to field-assisted exciton dissociation. However, the EQE_{PV} alone cannot reveal such a phenomenon since it is the product of several processes that are potentially bias-dependent, including CT state separation and charge extraction, the latter of which may be strongly hindered in the low-donor content blend studied. Nakano *et al.* investigated the photocurrent generation for several DA systems, varying the energy difference between the local singlet exciton (LE) and the CT state (expressed as the driving force $E_G{}^{opt-}E_{CT}$).[9] This study revealed a direct correlation between the efficiency of charge generation and $E_G{}^{opt-}E_{CT}$, highlighting the role of exciton dissociation. Importantly, not only free charge generation but also the ssPL became more bias-dependent with a smaller energy offset. It was proposed that the applied bias promotes the dissociation of the LE for systems with a small driving force. However, a bias dependence of ssPL does not necessarily imply that it originates from field-assisted exciton dissociation. For example, consider a situation where free charge carriers are either extracted to the electrodes (causing an external current) or recombine non-geminately through the reformation of the CT state. Since charge extraction is bias-dependent, so is the repopulation of CT states through non-geminate recombination. For low-offset systems, LE reformation from the CT state becomes efficient, whereby the LE and the CT states are in dynamic equilibrium.[10,11] As such, any bias dependence of the extraction-recombination equilibrium may cause equal changes of the LE (and CT) ssPL. More recently, Zou and co-workers performed TrPL and TAS on blends of the acceptor ICPDT-4F with three different donor polymers, thereby tuning the HOMO-HOMO-offset from 430 to −50 meV.[12] Although neither the TrPL nor the TAS kinetics was bias dependent for a high energy offset, the blends with small (or even negative) offset revealed an acceleration of the PL decay and an increase of the TAS signal assigned to free charge carriers with increasing reverse bias, and this was explained with an improved CT formation rate. However, none of these studies presented a quantitative comparison between the field-dependence of exciton dissociation and free charge generation, and the contribution of exciton reformation to PL emission was not addressed. Moreover, all these studies concerned only a small electric field range, and it remains to be answered whether photocurrent losses even remain at high reverse bias.

Here, we address these issues for the low-energetic offset blend of the donor polymer PM6 and the NFA Y5. This is a choice model system, due to the similarity in chemical and optical properties of the Y5 with the Y6 NFA, which enables a fair benchmark for comparison. We find that in contrast to PM6:Y6, the Y5-based blend exhibits a pronounced field-dependence of the photocurrent, meaning that it suffers from voltage-dependent recombination losses. By performing time-delayed collection (TDCF) experiments over a wide bias range, we identify field-dependent free charge generation rather than extraction losses as the leading cause of photocurrent loss. Artifacts due to dark-injected charge carriers[13] or fast recombination at interfaces[14] are ruled out by studying devices with different layer thicknesses and by utilizing a new modified TDCF (m-TDCF) technique. We then show that photoluminescence has the exact opposite bias-dependence as the free charge generation efficiency over the entire voltage range, from V_{OC} to −8 V reverse bias, proving that photocurrent generation is entirely governed by field-assisted exciton dissociation in the bulk of the material. At the same time, our study rules out a significant contribution from free charge carrier recombination to the bias-dependent ssPL.

II. RESULTS AND DISCUSSION

A. Chemical, optical, and optoelectronic properties

Figure 1(a) shows the chemical structure of the donor polymer PM6 and the NFA Y5, together with the energy levels taken from the literature.[3] Full chemical names of these moelcules are given in the supplementary material. Compared with Y6, Y5 exhibits a smaller offset of the HOMO to PM6, which is due to the absence of electron-withdrawing fluorene units on the terminals of the NFA. Figure 1(b) displays the absorption spectra of films of the neat components and the PM6:Yx blends. The absorption of neat Y5 is slightly blue-shifted compared with that of the popular Y6 NFA, although it is chemically similar in structure to its non-halogenated sibling. This suggests minor differences in intramolecular and intermolecular interactions. It has been shown that mainly molecular aggregates dominate the absorption in Y6 and chemically related Y-series NFAs in neat and blend films.[15] The absorbance of the optimized PM6:Y5 blend is not a perfect superposition of the neat NFA film's absorbance spectra, which we explain with slight differences in the molecular aggregation properties.

Our studies were performed primarily on PM6:Y5 devices in a conventional device geometry, using different electron transport layers (ETL) for different use cases, which we elucidate in later sections. Figure S1 (supplementary material) contains the averaged photovoltaic parameters for these device structures obtained from current-voltage (JV) characteristics. Optimized solar cells prepared with PM6:Y5 yield an open circuit voltage V_{OC} = 0.97 V, a short circuit current density J_{SC} = 15.5 mA/cm^2, and a fill factor FF = 55%. As expected from the smaller HOMO-HOMO offset, PM6:Y5 exhibits a higher V_{OC} than PM6:Y6. The significantly lower J_{SC} is more surprising, given the similar absorption properties of the PM6:Y5 and PM6:Y6 blend [Fig. 1(b)]. Finally, the relatively lower

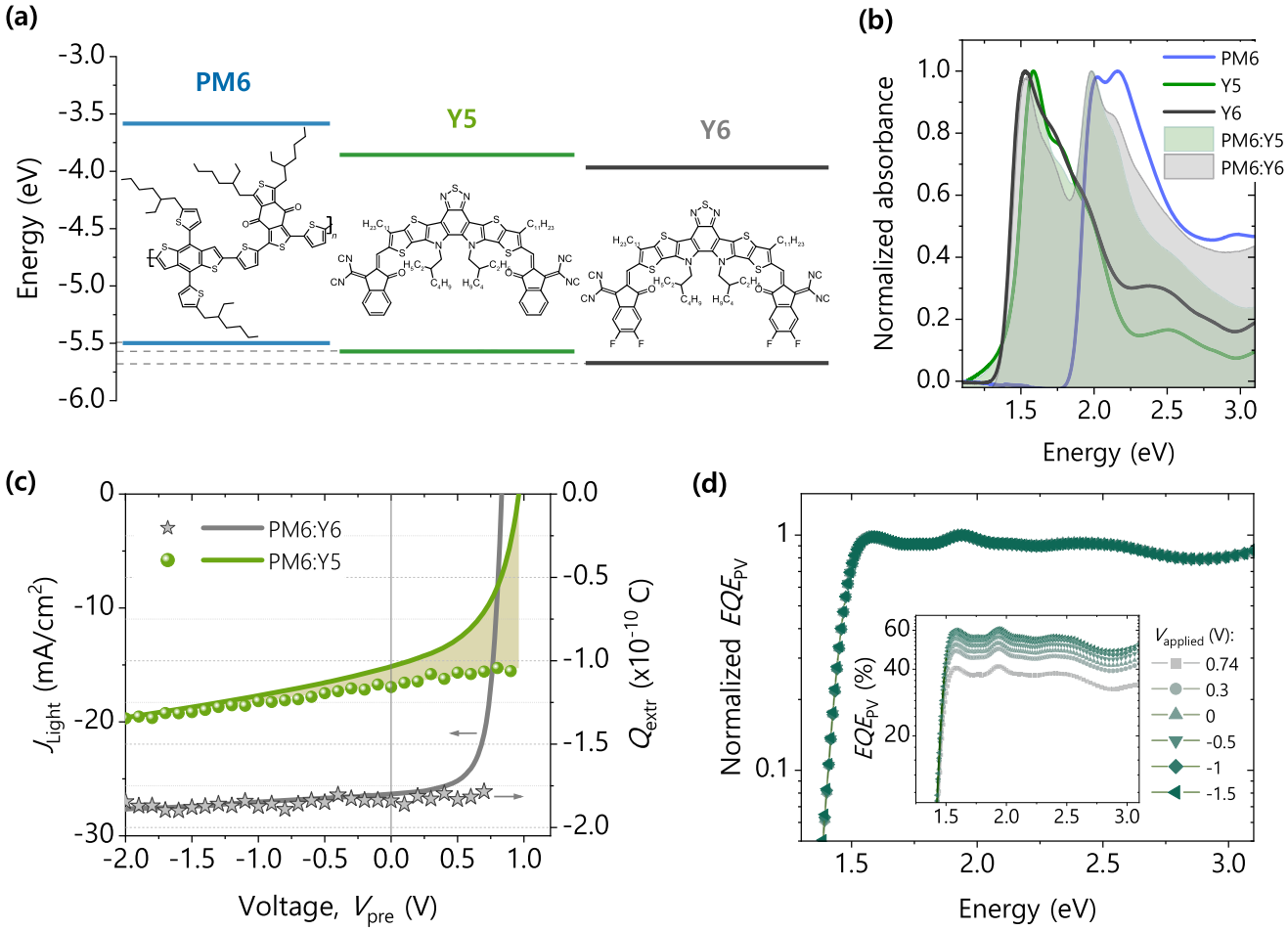

FIG. 1. A view of PM6:Y5 as a model system. (a) Chemical structures of PM6, Y5, and Y6 and energetics measured by cyclic voltammetry for the three organic molecules.[3] (b) Normalized absorbance of 110 nm neat/blend films (transmission mode). (c) Overlay of current-voltage (*JV*) characteristics measured under simulated AM1.5G light (solid line, left axis) and bias-dependent free charge formation from time-delayed collection field (TDCF) (symbols, right axis) for PM6:Y5 and PM6:Y6. In TDCF, the sample is excited with a 60 nJ/cm^2 fluence laser pulse of 2.33 eV, and the photogenerated free charge is extracted with a collection bias $V_{coll} = -2.5$ V. (d) Normalized EQE_{PV} as a function of bias for PM6:Y5, showing that the shape of the spectrum is independent of bias. The inset shows the unnormalized spectra.

FF hints at bias-dependent recombination losses, which are either geminate or non-geminate in nature or a combination of both.[16,17] Figure 1(d) shows the photovoltaic quantum efficiency (EQE_{PV}) as a function of the applied bias. As expected of a field-dependent system, a higher negative bias (increasing internal electric field) enhances the EQE_{PV}, but the normalized EQE_{PV} spectra overlap perfectly, as seen in Fig. 1(d). In other words, the process dictating field-dependent losses occurs independent of whether the PM6 or Y5 is initially excited.

To understand the reasons for this bias dependence, we performed time-delayed collection field measurements (TDCF) on PM6:Y5 and PM6:Y6 devices. TDCF is a powerful optoelectronic transient pump-probe method, which has been used previously to probe the generation, extraction, and recombination of free charge carriers in any solar cell device. The experimental details of the traditional TDCF technique are described in previous studies.[14,18,19] In essence, a full stack solar cell is held at a bias voltage (V_{pre}) during optical excitation with a ≈6 ns laser pulse. After the laser pulse, a negative bias voltage (V_{coll}) extracts all free charge carriers with a delay time of $t_{del,coll}$. If $t_{del,coll}$ is very short and a low fluence of optical excitation is chosen, then bimolecular non-geminate recombination of photogenerated charge carriers is nearly absent, and the bias-dependence of the extracted charge (Q_{extr}) measures the field-dependence of free charge generation. Figure 1(c) shows the results of these measurements for $t_{del,coll} = 1$ ns and a fluence of 60 nJ cm^{-2}. It is evident that PM6:Y5 suffers from field-dependent free charge generation, wherein the additional internal field provided by the pre-bias voltage assists in generating more free charge carriers. This is in contrast to PM6:Y6, in whose case free charge generation has been shown to be field-independent and barrier-less.[20] The difference between the bias-dependent TDCF and *JV* data at positive applied bias is assigned to non-geminate recombination (NGR), in part due to NGR between photogenerated charges carriers in the devices with dark-injected charge carriers from the electrodes.[14] Notably, this

difference is larger for the PM6:Y5 case, shown by the shaded area in Fig. 1(c), meaning that NGR is more severe. This will be addressed in a follow-up work.

Here, it should be noted that such fast NGR may also affect the result of TDCF measurements. One probable reason is the above-mentioned pseudo-first order NGR of photogenerated and dark-injected charge carriers.[21] Very high density of dark-injected charge carriers in the vicinity of ohmic contacts accelerates NGR rates, which can result in charge carrier losses even for small delays and fluences. This effect will be particularly pronounced for thin active layers and at V_{pre} close to the built-in voltage of the measured device. In fact, fast NGR in thin polymer:PCBM solar cells was experimentally shown to cause an apparent field-dependence of generation, and this was attributed to surface-related processes.[14] This issue will be addressed in the next two sections.

B. Ruling out artifacts in TDCF due to interface-related phenomena: TDCF experiments on different ETLs and sample thicknesses

As a first step to prove that the observed field-dependence of generation originates from processes within the bulk of the active layer, we performed TDCF measurements for (1) a range of active layer thicknesses and by (2) using two different perylene diimide-based ETLs, namely PDINO and PDINN (see supplementary material for more details). These different device stacks are illustrated in Fig. 2(a). Given the emphasis placed in these experiments on evaluating the effects of an electric field on generation processes in the active layer, one must be aware of the voltage drops across the different layers of the device. PDINN has been chosen here in comparison to the more common PDINO because its electrical conductivity (σ) of 6.4×10^{-3} Scm^{-1} is nearly two orders of magnitude higher than that in PDINO ($\sigma = 8.1 \times 10^{-5}$ Scm^{-1}). The electrical conductivities and doping concentrations of both ETLs were obtained using four-probe Van der Pauw measurements, see Fig. S2 (supplementary material). The higher conductivity of PDINN not only results in a small voltage drop but also a lower dielectric relaxation time, given by

$$\tau_d = \frac{\varepsilon_0 \varepsilon_r}{\sigma}. \quad (1)$$

Assuming that $\varepsilon_r = 3.5$, this yields $\tau_d = 48$ ps for PDINN vs ca. 6 ns for PDINO, which means faster redistribution of charge carriers within the PDINN layer in response to a change in the applied external bias. This is particularly beneficial for a transient technique such as TDCF where the applied bias is quickly switched from V_{pre} to V_{coll}

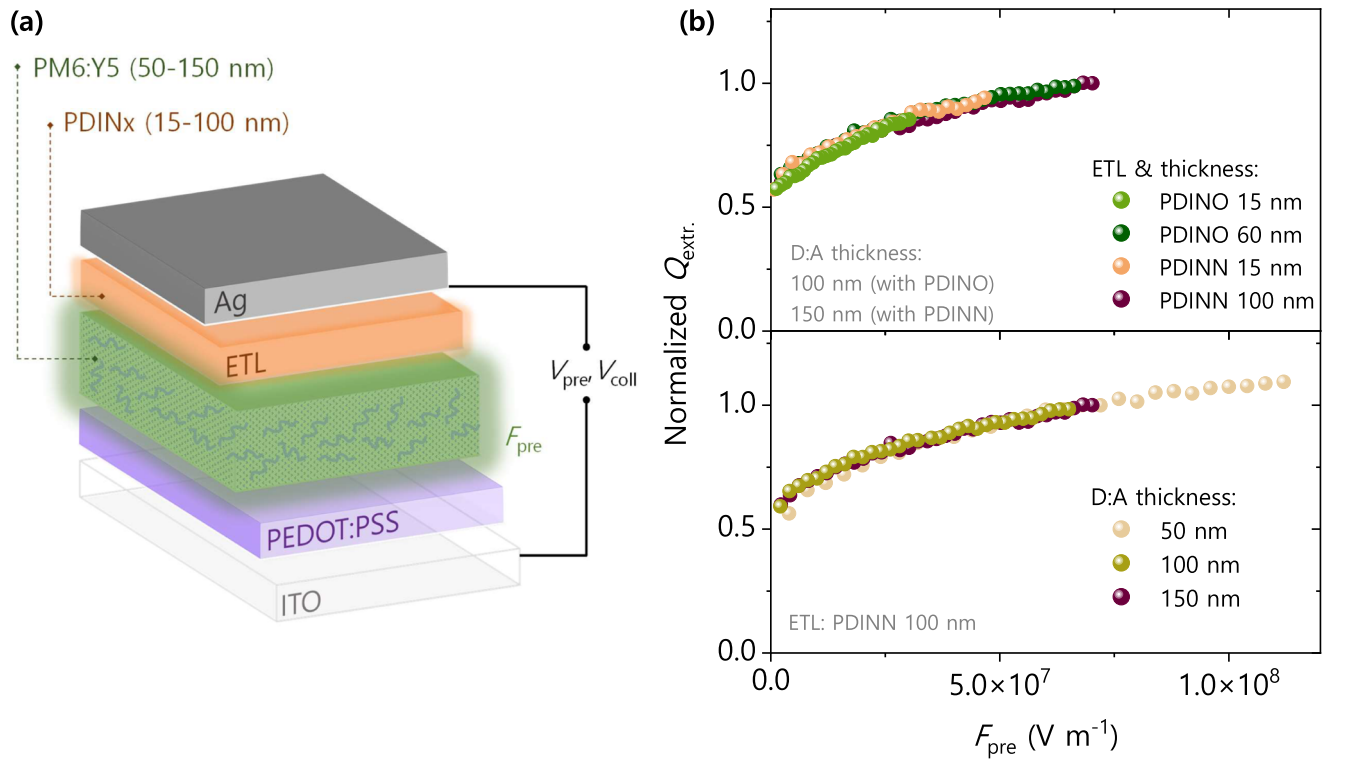

FIG. 2. Impact of the effective field on free charge generation in the bulk of the OPV active layer. (a) A schematic that illustrates the conventional PM6:Y5 device structure used in TDCF studies targeted at ruling out the contribution of interfacial phenomena to field-dependent free charge generation. The glow around the ETL and D:A layers signifies the field induced by the pre-bias, F_{pre}. By choosing a highly conductive ETL, F_{pre} is maximized across the PM6:Y5 layer that is beneficial for the efficient extraction of photogenerated charge carriers. (b) Extracted charge Q_{extr} normalized to a pre-bias field of 7×10^7 Vm^{-1} for (top panel) different ETL properties and (bottom panel) various PM6:Y5 layer thicknesses.

within a few nanoseconds. On the other hand, a higher free-electron concentration of PDINN would lead to a higher dark electron density in the active layer adjacent to the ETL ($N_{d,PDINN} = 6 \times 10^{18}$ cm^{-3} vs $N_{d,PDINO} = 2 \times 10^{17}$ cm^{-3}, see supplementary material. Further details will be published in a follow-up work). If the recombination of photogenerated holes with dark charge carriers affects the TDCF results, this would be visible by the comparison of TDCF data on devices using PDINN vs PDINO as the ETL.

The Q_{extr} against the pre-bias field (F_{pre}) for each device structure, normalized to $F_{pre} = 7 \times 10^7$ Vm^{-1}, is plotted in the top and bottom panels of Fig. 2(b). F_{pre} is calculated using the built-in voltage V_{bi} of the measured OPVs given by $F_{pre} = \frac{V_{bi} - V_{pre}}{d}$ (See Fig. S3 for the V_{OC} and V_{bi} values). Particularly good agreement of the data across all device structures implies that the field-dependence of extracted free charge generation remains unchanged, regardless of the active layer thickness and ETL, although PDINO and PDINN possess largely different transport properties. This gives sound evidence that the observed field-dependence of free charge generation is indeed a bulk phenomenon. Also, the overlap of data in the top panel of Fig. 2(b) means that the TDCF results are not altered by the higher doping concentration of PDINN or the slower redistribution of charge carriers in PDINO when applying the collection bias. We note that the field-dependence of free charge generation is gradual over the entire field range, characterized by a lack of saturation of Q_{extr} even at high field conditions above 1×10^8 Vm^{-1}. This is even more clearly seen in the semi-log representation of Fig. 2(b) in Fig. S3 (supplementary material). Interestingly, this observation deviates from the predictions of the Onsager-Braun model for CT separation, from which we expect a more sudden transition to the saturation regime for devices with fairly efficient zero-field charge separation, as seen here.[22]

C. Ruling out artifacts in TDCF due to the dark-injected charge carriers: Modified TDCF

Although the above data provide compelling evidence that field-dependent free charge generation originates in the bulk of the PM6:Y5 layer, we went one step further to specifically address the role of dark-injected charge carriers in the TDCF data. For this, a modified version of the TDCF technique is herein introduced (m-TDCF). Figure 3(a) succinctly illustrates different TDCF parameters and temporal characteristics of the photocurrent transients in both traditional and m-TDCF measurements. In traditional TDCF, the voltage transient returns to V_{pre} after extracting photogenerated charge carriers with V_{coll}. This means that for typical extraction times of 2–10 μs and a repetition rate of 500 Hz, the OPV is held at V_{pre} for almost 2 ms before being optically excited once again by the next laser pulse. This period is more than sufficient to establish steady-state conditions at the metal-semiconductor interface.

To cope with this, we have altered the shape of the applied voltage transient waveform. Within the same frequency of the laser pulse, the voltage transient in m-TDCF returns to 0 V instead of to V_{pre} after completion of the extraction time, as shown in Fig. 3(a). The voltage is then switched to V_{pre} for a short duration prior to and during illumination by the next laser pulse. The idea is to limit the duration of V_{pre} to just enough time for the OPV as a capacitor to become fully charged but well before a steady state dark condition is established. In Fig. 3(a), the delayed application of V_{coll} after the

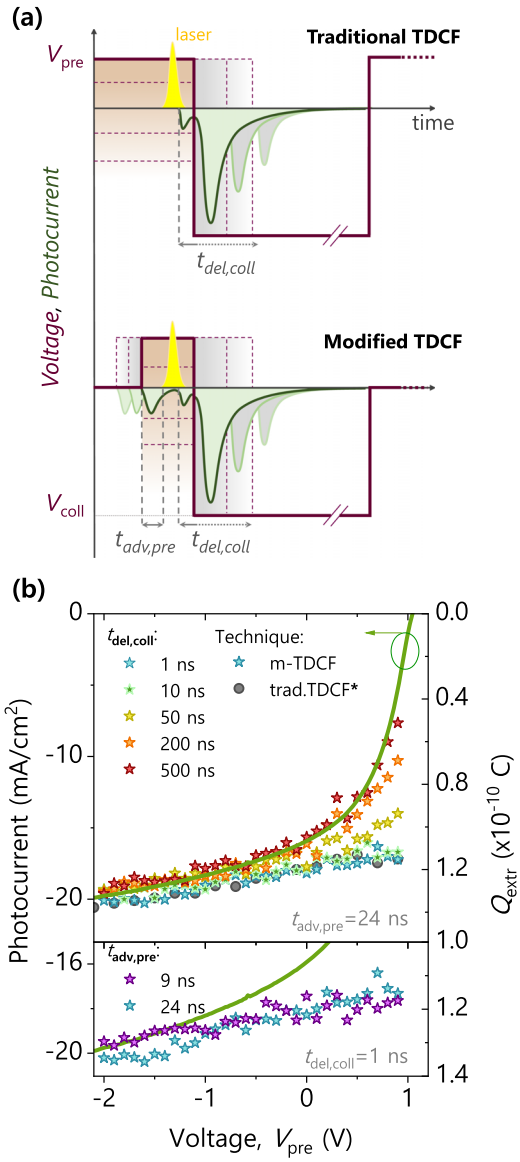

FIG. 3. Modified-TDCF (m-TDCF) measurements on PM6:Y5 for different delay settings. (a) An illustration of the temporal characteristics of both the traditional and the newly developed m-TDCF techniques. Voltage and photocurrent transients are shown in plum and green, respectively. The dotted lines depict voltage ranges and time scales of applying the pre-bias V_{pre} and collection bias V_{coll}. In contrast to traditional TDCF, the voltage waveform in m-TDCF returns to 0 V after complete charge extraction and switches to V_{pre} only shortly before the next laser pulse. Thereby, an additional temporal parameter $t_{adv,pre}$ defines how long the OPV is charged with V_{pre} prior to optical excitation. For different durations of $t_{del,coll}$ and $t_{adv,pre}$, the respective transient photocurrents are illustrated as translucent curves. (b) Measurement of m-TDCF on PM6:Y5 with a PDINN ETL. The photocurrent of PM6:Y5 from JV is overlaid on bias-dependent extracted charge obtained with m-TDCF, for a 2.33 eV laser excitation of 60 nJ/cm^2 fluence. The top and bottom panels show Q_{extr} for various $t_{del,coll}$ and $t_{adv,pre}$, respectively. Gray circles depict the bias dependence of the extracted free charge measured with traditional TDCF (*with $t_{del,coll}$ = 1 ns). A comparison is drawn to m-TDCF, where the collection delay is also 1 ns, and $t_{adv,pre}$ = 24 ns.

laser pulse is denoted by the parameter $t_{del,coll}$, and the time at which V_{pre} is applied prior to the laser pulse by the parameter $t_{adv,pre}$. To determine the optimum value for $t_{adv,pre}$, we take into account both the RC time of the OPV and the internal latency of the function generator that applies the voltage transient. For the measured PM6:Y5 OPVs, a pre-bias duration of $t_{adv,pre}$ = 24 ns is well suited for an active layer thickness of 110 nm, for which we found the RC time to be ~7 ns. The criteria to determine the optimal value for $t_{adv,pre}$ in this device are described in Fig. S4 in the supplementary material.

The upper panel of Fig. 3(b) shows Q_{extr} as a function of V_{pre} for $t_{adv,pre}$ = 24 ns and different $t_{del,coll}$ using the m-TDCF technique. We find that the bias dependence of Q_{extr} is the same for $t_{del,coll}$ = 1 ns and $t_{del,coll}$ = 10 ns. This rules out fast NGR losses prior to charge carrier extraction. We increased $t_{del,coll}$ even further to demonstrate the efficacy of the modified voltage waveform on reducing NGR near the electrodes. These data, shown for m-TDCF in Fig. 3(b), are compared with that from traditional TDCF in supplementary material, Fig. S5. As expected for longer $t_{del,coll}$, there are increasing charge carrier losses due to NGR not only among photogenerated charge carriers but also between photogenerated and dark-injected charge carriers. Eventually, at long enough extraction delays, the Q_{extr} from both TDCF techniques approaches the JV characteristics. Notably, NGR losses at longer $t_{del,coll}$ are enhanced in traditional TDCF compared with m-TDCF even for fairly fast collection ($t_{del,coll}$ = 10 ns) (see supplementary material, Fig. S5). This proves that the modified waveform in m-TDCF certainly reduces the presence of dark injected charge carriers available for NGR, by shortening the application of V_{pre}. We observe, importantly, that under optimum pre-bias delay and immediate extraction after laser excitation, the free charge generation recorded from traditional and m-TDCF overlap perfectly, seen in the upper panel of Fig. 3(b). This confirms that traditional TDCF measurements on PM6:Y5 are not affected by the injection of dark charge carriers over the entire voltage range (including at positive V_{pre}).

Finally, we note that if the delay between pre-bias application and photoexcitation is shorter than necessary to ensure the complete build-up of V_{pre} over the active layer, the apparent field dependence would be reduced. Indeed, by reducing the duration of $t_{adv,pre}$ from 24 to 9 ns and collecting the photogenerated charge carriers immediately after the laser pulse, the field dependence of free charge generation appears diminished, as seen by comparing the purple stars with the ideal delay condition in the lower panel of Fig. 3(b).

D. Interplay of photoluminescence and free charge generation

TDCF measurements on PM6:Y5 with different device structures and thicknesses and different voltage transients (TDCF vs m-TDCF), described earlier, provide comprehensive evidence for a pronounced field-dependence of free charge generation in the bulk of the active layer. This raises the question of whether it is inefficient (field-dependent) LE dissociation that mainly limits free-charge efficiency. To this end, we measured the intensity of steady-state photoluminescence as a function of bias, covering a wide electric field (F_{eff}) range up to 9 × 10^7 V m^{-1}. To benchmark the emission characteristics of PM6:Y5, we also measured the field-dependent ssPL of Y5 in an inert polystyrene (PS) polymer matrix. The comparison of the ssPL spectra of the PM6:Y5 blend with that of PS:Y5 shows that the blend emission is entirely controlled by the radiative decay of the Y5 LE for the same excitation wavelength (see Fig. S6a in the supplementary material). Also, the applied bias does not affect the shape of the ssPL spectrum (see Fig. S6b in the supplementary material). We find foremost that the peak photon flux ($\Phi_{ph,max}$) emitted from the PM6:Y5 device diminishes with increasingly negative bias (increasing electric field), suggesting that a stronger F_{eff} depletes populated LE states as emission channels, shown in Fig. 4(a). This is a clear indication of field-assisted exciton dissociation. However, given the smaller HOMO offset in PM6:Y5,

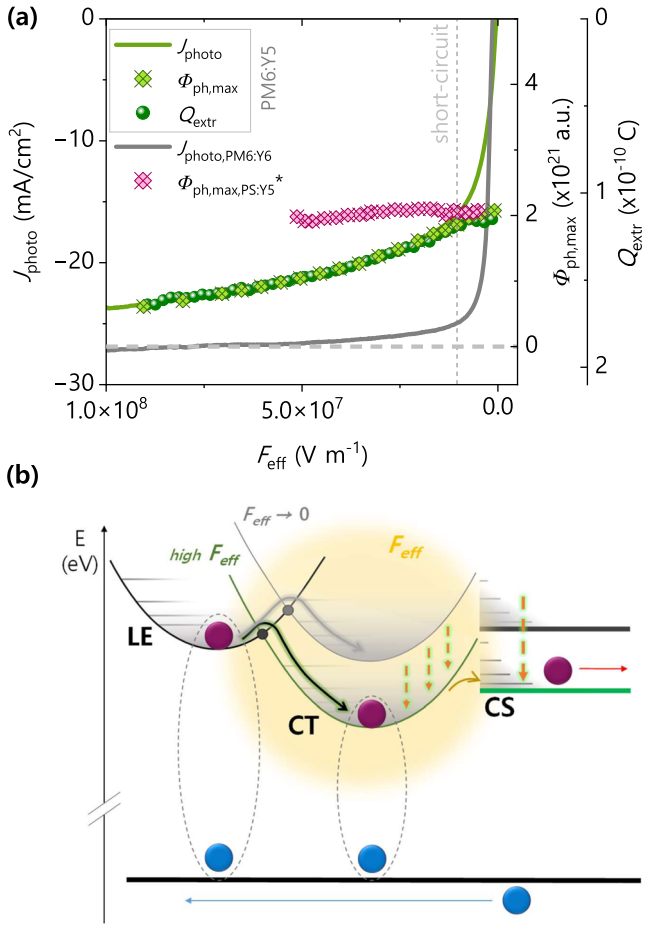

FIG. 4. Correlating photoluminescence and generation in PM6:Y5, benchmarked against PM6:Y6. (a) Overlay of the photocurrent (J_{photo}), Q_{extr} from traditional TDCF, and the peak ssPL photon flux $\Phi_{ph,max}$, all plotted as a function of the internal electric field for PM6:Y5 devices with a 110 nm active layer and a 15 nm PDINN ETL. Also shown is J_{photo} for PM6:Y6, and $\Phi_{ph,max}$ as a function of bias for a PS:Y5 blend with the same device structure (*the $\Phi_{ph,max}$ for PS:Y5 is scaled such that the emission intensity at V_{OC} matches that of the blend devices). The vertical dotted line marks the effective field F_{eff} at short-circuit conditions. (b) Marcus-type presentation of the potential curves of the local singlet exciton (LE) and the CT state. The application of an electric field (depicted by the yellow halo) reduces the energy of the CT state and thereby diminishes the barrier for the LE to CT transition. For simplicity, the energy of the CS state (and the CS state lowering due to the electric field) is indicated by horizontal lines.

LE reformation via the CT back transfer may serve as a competing pathway to LE dissociation. To assess the contribution of radiative decay from reformed LE excitons in the ssPL spectra, we recorded the PL quantum efficiency (PLQY) of the acceptor in PS and the EL quantum efficiency (ELQY) of the blend on full stack devices. We use the fact that the ratio of $ELQY_{PM6:Y5}$:$PLQY_{PS:Y5}$ gives a measure of what fraction of free charge carriers recombines radiatively by repopulating the NFA LE state at the interface in the blend.[23] Here, it is important that the PLQY is measured on the full solar cell stack for an accurate reformation efficiency. We therefore took special care to ensure that the excitation light in PLQY measurements illuminated only the OPV device area. The obtained values of $PLQY_{PS:Y5} = 2.5 \times 10^{-2}$ and $ELQY_{PM6:Y5} = 2.2 \times 10^{-3}$ show that emission from repopulated LE states accounts for not more than ~9% of the total emission. Moreover, any reformed LE states may dissociate again under the effect of a large internal field, which depletes the LE emission channel.

Figure 4(a) shows the J_{photo}, $\Phi_{ph,max}$, and Q_{extr} for PM6:Y5, all measured up to high F_{eff}. In addition, the J_{photo} of the prototypical PM6:Y6 OPV is plotted for the same field range. Since both PM6:Y5 and PM6:Y6 blends exhibit similar absorption spectra, it must follow that the exciton generation rates in the two blends are comparable. This, paired with activation-less free charge generation exhibited by PM6:Y6, lets us presume that the reverse saturation of J_{photo} in PM6:Y6 represents the situation where (nearly) all NFA excitons dissociate into CT states and finally into free charges, i.e., where free charge generation proceeds with nearly no activation barrier. We first note that at sufficiently high F_{eff}, the J_{photo} of the poorly performing PM6:Y5 OPV approaches the J_{SC} of PM6:Y6 ($J_{high\text{-}field,PM6:Y5}$ = 24.1 mA/cm^2 vs $J_{SC,PM6:Y6}$ = 24.9 mA/cm^2). This means that almost all excitons generated in PM6:Y5 can eventually dissociate under a sufficiently high F_{eff} and contribute to the photocurrent. The lack of saturation of J_{photo} even at a F_{eff} approaching 1×10^8 V m^{-1} suggests that a small barrier for LE or CT dissociation still exists under high fields. Furthermore, it turns out that Q_{extr} from TDCF can be perfectly superimposed on J_{photo} at a high reverse bias (high F_{eff}); indicating the region where the field dependence of J_{photo} is completely described by the field dependence of free charge generation, with vanishingly low free charge carrier recombination. We now correlate the J_{photo} and Q_{extr} datasets with $\Phi_{ph,max}$ from field-dependent ssPL spectra. We find that (a) the $\Phi_{ph,max}$ of PM6:Y5 can be completely overlaid on the Q_{extr} data over the entire field range and (b) that for this scaling a zero ssPL intensity corresponds to the reverse saturation photocurrent of PM6:Y6—where there is no barrier for exciton dissociation. This explains the importance of the gray horizontal dashed-line in Fig. 4(a). The fact that there is little deviation between $\Phi_{ph,max}$ and Q_{extr} even near V_{OC}, where photocurrent loss is mainly due to NGR, supports our early assignment that the ssPL has little contribution from exciton reformation due to free charge carrier recombination.

At this point, the question arises as to whether the observed field dependence of LE dissociation is that of LE states generated in the bulk of neat Y5 domains or whether it is an interfacial phenomenon, i.e., it only helps to overcome a barrier toward CT formation. For this, we compare $\Phi_{ph,max}$ vs bias for PS:Y5 devices with that of PM6:Y5 devices with the same device geometry, shown in Fig. 4(a). The peak PL photon flux is field independent in the PS:Y5 case, which highlights the fact that the effective internal field only affects exciton dissociation at the DA heterojunction, i.e., formation of interfacial CT states. Such a scenario requires that an appreciable energetic barrier exists between LE and CT states, which is indeed predicted by the Marcus theory for the case of a small energetic offset and an appreciable reorganization energy.[24] This situation is depicted in Fig. 4(b). The effect of F_{eff} lowers the CT state energy that, in turn, reduces the barrier toward CT state formation. A sizeable field-induced lowering of this barrier requires the CT to carry a large electric dipole moment and/or to be highly polarizable.[25] Significant charge delocalization of the CT state has been predicted recently for the prototypical NFA Y6, which could explain a large dipole moment for the excited CT state.[26] Such effects could also be applicable to Y5-based blends, due to the similar NFA chemical structure.

In conclusion, we studied the interrelation between free charge generation and exciton decay in optimized blends of the polymer donor PM6 with the Y5 NFA, a non-halogenated sibling of the NFA Y6, albeit exhibiting a lower HOMO-HOMO offset with the polymer donor. We developed a new TDCF method called m-TDCF to prove the absence of recombination-induced artifacts in the experimental free charge generation data. By systematically studying devices with different active layer thicknesses and with two different ETLs, the field-assisted process is revealed to be a bulk phenomenon. Finally, we show that the field dependencies of free charge generation and photoluminescence intensity are perfectly anticorrelated, with zero emission intensity corresponding to the case of complete exciton dissociation. These findings clearly point to insufficient LE dissociation as the limiting factor for photocurrent generation in this system. Our approach can be used to analyze the field dependence of other NFA-based systems, which are currently being studied to obtain an eagle's eye view on free charge generation in low energetic offset NFA-based OPVs.

SUPPLEMENTARY MATERIAL

Experimental methods describing fabrication and experimental techniques used; Figs. S1–S6 showing JV curve for optimized PM6:Y5 with statistics, conductivity of ETLs, semi-log of extracted charge for different device structures to show bulk origin of field-dependent generation, snapshot of photocurrent transient and explained determination of $t_{adv,pre}$ in modified-TDCF, JV and Q_{extr} for delayed extraction in traditional vs modified TDCF, and PL (OC) comparison for PS:Y5 and PM6:Y5 devices and bias dependent PL spectra for PM6:Y5.

ACKNOWLEDGMENTS

We thank the Deutsche Forschungsgemeinschaft (DFG, German Research Foundation) for funding through the project Extraordinaire (Project No. 460766640). Publication funded by the Deutsche Forschungsgemeinschaft (DFG, German Research Foundation) – Project No. 491466077. Dr. Musiienko thanks funding received from the European Union's Framework Programme for Research and Innovation HORIZON EUROPE (2021-2027) under the Marie Skłodowska-Curie Action Postdoctoral Fellowships (European Fellowship) 101061809 HyPerGreen.

AUTHOR DECLARATIONS

Conflict of Interest

The authors have no conflicts to disclose.

Author Contributions

Manasi Pranav: Conceptualization (equal); Data curation (lead); Formal analysis (equal); Investigation (equal); Visualization (lead); Writing – original draft (lead); Writing – review & editing (equal). **Thomas Hultzsch**: Methodology (equal); Software (lead). **Artem Musiienko**: Data curation (supporting); Writing – review & editing (supporting). **Bowen Sun**: Writing – review & editing (supporting). **Atul Shukla**: Writing – review & editing (supporting). **Frank Jaiser**: Methodology (supporting). **Safa Shoaee**: Supervision (supporting); Writing – review & editing (supporting). **Dieter Neher**: Conceptualization (equal); Formal analysis (equal); Funding acquisition (equal); Investigation (equal); Supervision (equal); Writing – original draft (supporting); Writing – review & editing (equal).

DATA AVAILABILITY

The data that support the findings of this study are available within the article and its supplementary material.

REFERENCES

[1]Y. Dong *et al.*, "The binding energy and dynamics of charge-transfer states in organic photovoltaics with low driving force for charge separation," J. Chem. Phys. **150**(10), 104704 (2019).
[2]M. Saladina *et al.*, "Charge photogeneration in non-fullerene organic solar cells: Influence of excess energy and electrostatic interactions," Adv. Funct. Mater. **31**(8), 2007479 (2021).
[3]J. Bertrandie *et al.*, "The energy level conundrum of organic semiconductors in solar cells," Adv. Mater. **34**(35), 2202575 (2022).
[4]J. Zhang *et al.*, "Accurate determination of the minimum HOMO offset for efficient charge generation using organic semiconducting alloys," Adv. Energy Mater. **10**(5), 1903298 (2020).
[5]A. Karki *et al.*, "The role of bulk and interfacial morphology in charge generation, recombination, and extraction in non-fullerene acceptor organic solar cells," Energy Environ. Sci. **13**(10), 3679–3692 (2020).
[6]A. Classen *et al.*, "The role of exciton lifetime for charge generation in organic solar cells at negligible energy-level offsets," Nat. Energy **5**(9), 711–719 (2020).
[7]Y. Liu *et al.*, "Electric field facilitating hole transfer in non-fullerene organic solar cells with a negative HOMO offset," J. Phys. Chem. C **124**(28), 15132–15139 (2020).
[8]A. Weu *et al.*, "Field-assisted exciton dissociation in highly efficient PffBT4T-2OD:fullerene organic solar cells," Chem. Mater. **30**(8), 2660–2667 (2018).
[9]K. Nakano *et al.*, "Anatomy of the energetic driving force for charge generation in organic solar cells," Nat. Commun. **10**(1), 2520 (2019).
[10]F. D. Eisner *et al.*, "Hybridization of local exciton and charge-transfer states reduces nonradiative voltage losses in organic solar cells," J. Am. Chem. Soc. **141**(15), 6362–6374 (2019).
[11]O. J. Sandberg and A. Armin, "Energetics and kinetics requirements for organic solar cells to break the 20% power conversion efficiency barrier," J. Phys. Chem. C **125**(28), 15590–15598 (2021).
[12]X. Zou *et al.*, "Optically probing field-dependent charge dynamics in non-fullerene organic photovoltaics with small interfacial energy offsets," J. Phys. Chem. C **125**, 1714 (2021).
[13]S. Schiefer *et al.*, "Determination of the intrinsic and the injection dependent charge carrier density in organic solar cells using the Suns-V_{OC} method," J. Appl. Phys. **115**(4), 044506 (2014).
[14]J. Kurpiers and D. Neher, "Dispersive non-geminate recombination in an amorphous polymer:fullerene blend," Sci. Rep. **6**, 26832 (2016).
[15]D. Kroh *et al.*, "Identifying the signatures of intermolecular interactions in blends of PM6 with Y6 and N4 using absorption spectroscopy," Adv. Funct. Mater. **32**(44), 2205711 (2022).
[16]D. Bartesaghi *et al.*, "Competition between recombination and extraction of free charges determines the fill factor of organic solar cells," Nat. Commun. **6**, 7083 (2015).
[17]R. Mauer, I. A. Howard, and F. Laquai, "Effect of nongeminate recombination on fill factor in polythiophene/methanofullerene organic solar cells," J. Phys. Chem. Lett. **1**, 3500 (2010).
[18]J. Kurpiers *et al.*, "Probing the pathways of free charge generation in organic bulk heterojunction solar cells," Nat. Commun. **9**(1), 2038 (2018).
[19]J. Kniepert *et al.*, "A Conclusive view on charge generation, recombination, and extraction in as-prepared and annealed P3HT:PCBM Blends: Combined experimental and simulation work," Adv. Energy Mater. **4**(7), 1301401 (2014).
[20]L. Perdigón-Toro *et al.*, "Barrierless free charge generation in the high-performance PM6:Y6 bulk heterojunction non-fullerene solar cell," Adv. Mater. **32**(9), 1906763 (2020).
[21]U. Würfel and M. Unmüssig, "Apparent field-dependence of the charge carrier generation in organic solar cells as a result of (bimolecular) recombination," Sol. RRL **2**(10), 1800229 (2018).
[22]C. L. Braun, "Electric field assisted dissociation of charge transfer states as a mechanism of photocarrier production," J. Chem. Phys. **80**(9), 4157–4161 (1984).
[23]L. Perdigón-Toro *et al.*, "Excitons dominate the emission from PM6:Y6 solar cells, but this does not help the open-circuit voltage of the device," ACS Energy Lett. **6**(2), 557–564 (2021).
[24]R. A. Marcus, "On the theory of oxidation-reduction reactions involving electron transfer. I," J. Chem. Phys. **24**(5), 966 (1956).
[25]C. Poelking and D. Andrienko, "Design rules for organic donor-acceptor heterojunctions: Pathway for charge splitting and detrapping," J. Am. Chem. Soc. **137**(19), 6320–6326 (2015).
[26]G. Zhang *et al.*, "Delocalization of exciton and electron wavefunction in non-fullerene acceptor molecules enables efficient organic solar cells," Nat. Commun. **11**(1), 3943 (2020).